Microfluidic Mixing by dc and ac Nonlinear Electrokinetic Vortex Flows

Shau-Chun Wang[†] and Yi-Wen Lai

Department of Chemistry and Biochemistry, National Chung Cheng University, 160 San Hsing, Ming Hsiung, Chia Yi 621, Taiwan

Yuxing Ben[†] and Hsueh-Chia Chang*[,†]

Department of Chemical and Biomolecular Engineering, University of Notre Dame, Notre Dame, Indiana 46556

A novel micromixing strategy is proposed for microfluidic applications. High-intensity nonlinear electroosmotic microvortices, with angular speeds in excess of 1 cm/s, are generated around a small (∼1 mm) conductive ion-exchange granule when moderate dc and ac electric fields (30−125 V/cm) are applied across a miniature chamber smaller than 10 μL. Coupling between these microvortices and the fast electrophoretic motion (∼1 cm/s) of the granule in low frequency (between 0.3 and 1.0 Hz) ac fields and a slower backflow vortex (velocity ∼1 mm/s) in dc fields produces an intense chaotic micromixing action. Two segregated dye samples, normally requiring nearly 0.5 h to mix by diffusion, are observed to mix within 30 s in the mixing chamber. The effective diffusivity scales as E^2 and is measured to be 2 orders of magnitude higher than molecular diffusivity at reasonable field strengths and optimal frequencies. The main vortices are generated by nonlinear versions of the Smoluchowski slip velocity on the granule surface that result from a nonuniform counterion flux into the granule and the corresponding nonuniform polarization. Although these nonlinear electrokinetic vortices cease after 30 min as the granule saturates with the counterions, this mixing chamber should prove useful for mixing aqueous/electrolyte samples in disposable microchips and in batch microreactors. Mixing by ac field is preferred because of the solute can be better confined within the mixing chamber and contamination by electrode reaction is reduced.

Introduction

Despite the small dimensions of microfluidic devices, mixing by diffusion still requires an unacceptably long time. For example, for low analyte diffusion coefficients of $D = 10^{-7}$ cm^2/s (for protein and many biomolecules), the docking time $t = l^2/D$ within a $l = 200$ μm wide channel is still 0.5 h. This docking transport time is typically longer than the reaction time scale, and the overall reaction process is hence transport (diffusion) limited. For wet wells in high-throughput drug screening with a linear dimension l of 1 mm, the diffusion time is even longer, often in excess of 1 h. This slow transport time scale has become a bottleneck for many high-throughput tests using wet wells or microfluidic biochips. Any reduction in the transport time would then produce a corresponding increase in the throughput.

There have hence been many recent efforts to fabricate micromixing chambers to overcome the diffusion limitation. Unlike micromixers, the miniscule Reynolds numbers ($Re < 0.1$) of most microfluidic flows imply that turbulent mixing with transient vortices of all length scales is not available. Static mixers often use a flow splitting (multilamina) technique[1,2] to reduce the diffusion length l or employ obliquely oriented grooves to enhance transverse components in flows. However, reduction of l below 100 μm requires fabrication of microsplitters and microbaffles in a long mixing channel, which is time and labor intensive. Such baffles are also problematic in chips that employ electroosmosis or electrophoresis as high fields occur near sharp corners. As a result, the stagnant regions within the baffle often cause protein precipitation and colloid aggregation.[3] Microstirrers and other mixers with moving parts suffer from even more severe fabrication difficulties.

For electrokinetic microdevices, several simple mixing strategies have appeared. An apparent electrokinetic mixing instability has been observed in a high-field (10^3 V/cm) and low-frequency (20 Hz) ac field.[4] However, it is difficult to use such a high field in biological analysis. Besides, the mixing intensity of these electrokinetic mechanisms, as measured by the velocity of the vortices, is typically of the order of the electroosmotic velocity at the applied field.[5] With typical fields of 100 V/cm in practical electrokinetic devices, the electroosmotic velocity is less than 1 mm/s and the mixing intensity is also correspondingly low.

Nonlinear Electrokinetics

In fact, mixing vortices are difficult to induce in standard electroosmotic flow with uniform ζ potential and without any spurious instability. In the Debye layer near the surface, the intense normal electric field created by surface charges would attract the counterions and repel the co-ions. However, because there is no ion flux into the solid or out of it, both ions form equilibrium

* To whom correspondence should be addressed. Tel.: (574) 631-5697. Fax: (574) 631-8366. E-mail: chang.2@nd.edu.

[†] Present address: Center for Microfluidics and Medical Diagnostics, University of Notre Dame, Notre Dame, IN 46556.

10.1021/ie030689r CCC: $27.50
Published on Web 03/30/2004

Boltzmann distributions within the thin Debye layer of less than 100 nm. These ions screen the electric field of the surface charges such that the electric potential drops precipitously away from the wall in the Debye layer to produce a potential drop corresponding to the ζ potential. When a tangential field is applied over the surface, the Maxwell stress on the electrolyte is confined to the thin polarized Debye layer where there is a net charge. A simple momentum balance then stipulates that the slip velocity (the Smoluchowski slip) near the surface due to this Maxwell force is proportional to the tangential field E with the ζ potential a part of the proportionality constant $u_s = -\epsilon E\zeta/\eta$.[6] If the ζ potential is constant everywhere and if there is no internal pressure gradient, the proportionality between the velocity field and the electric field (gradient of the potential) holds everywhere in the device—the field lines coincide. This means that, under these conditions, the flow in the ohmic region is a potential flow proportional to the electric field, i.e., the gradient of the potential. A potential flow has zero vorticity (it is irrotational with zero curl), and this rules out the existence of vortices in standard electroosmotic flow.

A unique nonlinear version of electrokinetic flow that revokes the irrotational character was recently predicted by Dukhin[7] and later verified experimentally by Mishchuk and Takhistov.[8] Such flows exist near a conducting ion-selective granule in a uniform electric field within an electrolyte. Because of the flux of counterions into the granule, the counterion distribution is no longer Boltzmann. In fact, to sustain this flux of counterions, there must be a diffusive normal concentration gradient outside the polarized layer where the surface field has been completely screened. Because of near complete screening outside the Debye layer, the normal field is very weak there and the resulting counterion electromigration cannot replenish the flux without the concentration gradient.

This concentration gradient due to ion flux creates a unique ion depletion layer right outside the Debye layer. Without tangential electroosmotic flow effects (low Peclet numbers), this gradient eventually vanishes about a distance of the granule radius from the surface.[9] The diffusion layer where the gradient persists is essentially that created by diffusion from the surrounding electrolyte with a homogeneous concentration to the spherical granule with a nearly zero concentration. With large tangential convection due to electroosmotic flow (large Peclet number), a hydrodynamic diffusion layer exists around the granule whose thickness is roughly the granule radius multiplied by the $-1/2$ power of the Peclet number.[9,10] The thickness of the depletion layer is controlled by the diffusion boundary layer, created by either pure diffusion or convection and diffusion around the granule. It typically ranges from 1 to 10 μm, or as much as 10 times the original equilibrium Debye layer without ion flux.

As the co-ion must still have a lower concentration than the counterion in this depletion layer, its net charge is still nonzero even though both concentrations have been depleted. As a result, the thick depletion layer created by ion flux is a secondary polarized layer with space charges. It extends the polarized region from the original thin equilibrium Debye layer into the thick diffusion layer. Because of this long charged depletion layer with low conductivity, the potential drop from the surface to the bulk (called the effective ζ potential, ζ_{eff}), across both the polarized Debye layer and the depletion layer, exceeds the ζ potential of a granule without ion flux by several factors.

Moreover, the effective potential and the thickness of this depletion layer are both proportional to the normal electromigration flux of counterions; i.e., it is proportional to the normal component of the applied electric field. Because the Smoluchowski velocity is proportional to the product of the overpotential to the applied tangential field, the velocity now scales as the square of the applied field rather than the linear scaling of the standard electroosmosis.

Dukhin[7] first offered an estimate of this unique nonlinear electroosmostic flow. Because the counterions only enter one side of the granule, the other side does not possess an insulating depletion layer and is in good electric contact with the electrolyte. The surface electrolyte potential on the side without counterion flux is hence equal to the potential of the high-conductivity granule, which can be set to zero as a reference. However, the depletion layer and the extended polarized region on the side with counterion flux essentially electrically separate the electrolyte from the granule. As a result, the electrolyte electric field on this side is tangential to granule. The Ohmic potential drop Φ along this circumferential field line hence increases from zero at the equator (where the two halves of the granule meet) to $E\pi a/2$ at the pole aligned with the external field, where E is the applied field and a the granule radius. Because the granule has zero potential, the effective ζ potential for the ion-exchange granule is then $\Phi(\theta) = [(E\pi \sin \theta)/2]a$, where θ is measured from the equator. Unlike the ζ potential of linear electrokinetics, which results from the screening of surface field by cloud charges, this effective ζ potential due to screening of external field by the extended polarized layer is position dependent and proportional to the applied field.

Using the average ζ potential,

$$\langle \zeta_{eff} \rangle = Ea \tag{1}$$

as an estimate, Dukhin's estimate of the average nonlinear electroosmotic velocity is then

$$\langle u_s \rangle = -\epsilon E^2 a/\eta \tag{2}$$

For larger granules (a > 1 mm) and typical fields (<100 V/cm), the average potential drop ranges from 1 to 10 V, far larger than typical ζ potential of 100 mV. We hence expect the nonlinear electrokinetic velocity, which is size dependent and scales as E^2, to be 10−100 times larger than linear electrokinetics. This immediately offers much faster electrophoretic and mixing motion unavailable from linear electrokinetics. We[9,10] have recently extended Dukhin's theory to include partial insulation and large Peclet diffusion layer effects. The resulting average velocity is less than Dukhin's estimate (2) but is still orders of magnitude higher than linear electrokinetics.

Banary et al.[11] have indeed measured nonlinear electrokinetic velocities in excess of 1 cm/s or 10−100 times larger than standard electroosmotic velocity. The velocity field also naturally exhibits vortices as the overpotential is nonuniform around the granule.[10] At the poles where the normal field is highest the polarized layer can be as thick as 10 μm and ζ_{eff} exceeds 1 V for a 1 mm granule on a 50 V/cm field. This ζ_{eff} is at least 10 times higher than normal ζ potentials at 50 mV.

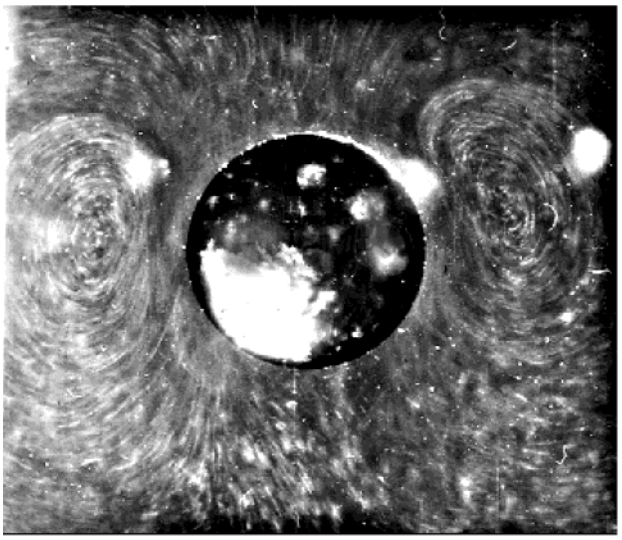

Figure 1. Closed vortex pair imaged with multiexposure imaging for a cation-exchange granule in a large reservoir. The streamlines are images of small particles in the flow. The 50 V/cm field is applied from the top where the pole is located, and the vortices are typically seen only on the side facing the field where there is a cation flux. The vortex flow on the side of the surface is from the pole to the equator (in the direction of the field) for a cation-exchange granule. (The opposite is true for an anion-exchange granule.) Some apparent downward shift of the vortices to the equator occurs because of granule motion. The estimate of the particle velocity at the vortex is about 2 cm/s.

Most significantly is the possibility of vortex formation absent in linear electrokinetics. This large ζ_{eff} decays toward the equator where the normal field vanishes. The tangential Maxwell stress in the extended depletion and Debye layers at the pole can be 1 or 2 orders of magnitude higher than that of a surface-charge-generated Debye layer at the equator. As is consistent with Barany et al.'s measurements,[11] our estimate of electroosmotic velocity at the granular pole can reach several cm/s at a moderate field of 50 V/cm. Moreover, because ζ_{eff} is nonuniform around the granule with a large flow at the pole into the equator region with low flow, a pressure gradient develops near the granule to produce backflow and ensure flow balance. Because the velocity near the granule is still the slip velocity due to the Maxwell stress in the polarized region, the backflow occurs further away from the surface. As a result, large and intense electroosmotic vortices are produced near a stationary granule and are ideal for micromixing applications. The mixing vortices are now 10−100 times more intense at several cm/s for a moderate field of 50 V/cm. An image of the vortices is shown in Figure 1.

Mixing Vortices

In this report, we exploit these highly nonlinear and intense electrokinetic vortices to fabricate a simple but effective mixing chamber. The mixing requires an applied electric field. It is hence quite easy to integrate this chamber into an electrokinetic microdevice. However, even for pressure-driven electrolyte flow in microdevices, the electric field can be applied with local electrodes imbedded within the device. The nonlinear electrokinetic action stops after about 30 min when the granule is saturated with counterions. Regeneration is possible but the chamber is probably most suitable for disposable chips. Another potential application is for reagents in wet well arrays that are dispensed by a micropipet array, as will be discussed subsequently.

Although the vortices in Figure 1 are intense, they are smaller than the granule size of 1 mm. Hence, solutes from the rest of the reservoir must diffuse slowly in and out of their closed streamlines to be mixed, which is extremely slow. Hence, the mixing can be significantly improved if the closed streamlines are broken by another flow field. This secondary flow does not need to be fast to significantly enhance the mixing efficiency. In a related heat-transfer problem,[14] we have shown an order-of-magnitude improvement with a slow secondary flow that breaks the closed streamlines of vortices. Two such secondary flows will be introduced in our mixing chamber design. The granule will be induced to rattle electrophoretically with an ac field. A slow pH-induced backflow (<1 mm/s) will also be produced with a dc field to break the closed streamlines of the nonlinear electrokinetic vortices of Figure 1.

As discussed previously, the thickness of the flux-induced polarization layer is 1−10 μm. In other words, ions need 10^{-3}−10^{-1} s to diffuse across this length scale and establish the steady-state polarized layer. Another important time scale is the translation time of granule across the reservoir which, for a reservoir of about 3 mm in diameter, is about 1−10 s. These time scales are irrelevant for dc mixing action. However, they are important with an ac field. If the applied field has a period much less than the diffusion time, counterions cannot be driven into the granule and polarization cannot take place. The granule rattling around the reservoir helps to complete mixing. This rattle disappears for an ac frequency less than the inverse of granule translation time. There should hence be maximum mixing at an optimum frequency which will be investigated.

Experimental Section

Vivak copolyester thermoplastic sheets are obtained from Sheffield Plastics Inc. (Sheffield, NJ). Cation and anion-exchange granules from Bayer are activated with dilute hydrochloric acid and NaOH solutions, and both are kept in deionized waters before they are used. Blue and red miscible commercial food color is used as dye without any pretreatment. The diffusion coefficient of the food dye is estimated to be 1 order of magnitude smaller than that of small molecules (less than 1000 Da). The dye is used to visualize flow, and it is selected on the basis of the charge to prevent its penetration into the granule. Such penetration tends to reduce the flux of counterions and the intensity of the vortices. For cation-exchange granules, we use a negatively charge dye Rhodamine-6G, and for anion-exchange granule, a positively charged methylene blue dye is used. Glycerin reagents used in this study for quantitative mixing characterization are from Sigma. These glycerin solutions are colored by the dye in a separate flask, and microliter droplets of them are retrieved and placed in the mixing reservoir for visualization in a manner to be described subsequently.

To minimize bubble generation and joule heating, which tend to generate mixing action of their own, we house the positive and negative electrodes in the two outer reservoirs of the specific configuration shown in Figure 2, with the anode at the top and the cathode at the bottom. These outer reservoirs are connected by two straight channels to a center reservoir between them.

Figure 2. Schematic of the reservoir-channel setup. The anode is place at the top reservoir, and the cathode, at the bottom reservoir. The black ball in the middle reservoir is a cation-exchange resin. Two negatively charged dyes with different colors shown as the shadow are dropped in the middle reservoir. The electrophoretic motion of the dye is toward the top reservoir with the anode. Some leakage of the dye in that direction is evident.

The colored glycerin droplets (red and green) are placed and mixed in the central reservoir. All three reservoirs are 3 mm in diameter and are drilled on a thermoplastic slide (20 mm × 40 mm; 1 mm in thickness). The connecting channels are 1.0 mm in width, which is slightly narrower than the 1.2 mm granule, and each segment between the two reservoirs is 12 mm long. The holes and grooves are machined on a plastic slide with conventional drilling and milling tools. The substrate slide is then thermally bonded to the drilled one. Pressure is briefly applied using binder clips to glue the slides together at a temperature of 80−100 °C, which is higher than the plastic softening temperature (75 °C). Electrodes of stainless steel are placed in two side-reservoirs. Stainless steel strips (1 mm × 20 mm) are taped onto the slides. Their tips are bent to dip into the reservoirs to make contact with the liquids. Some bubbles are formed at the side reservoirs, but they rise to the surface without migrating into the center reservoir. There is hence little mixing due to bubble generation. Thermal convection due to joule heating is also not observed in the center reservoir.

One granule (approximately 1.2 mm in diameter) is placed inside the center reservoir prior to the experiment. Small dc voltages are generated with a power supply in the range of 100−450 mV. The ac waveforms (−450 to +450 mV; duty cycle 50%) are provided by a functional generator (0.1 Hz to 50 kHz) and are amplified to 1000 times with a high-voltage amplifier (Trek 10/10).

For dc mixing experiments, one cation-exchange granule (approximately 1.2 mm in diameter) is placed inside the center reservoir prior to the experiment. Reservoirs and channels are then filled with deionized water. One drop of each color dye is stained on a thin metal wire tip. Two wire tips are dipped into the center reservoir as the external voltage is applied. The electric field within the center reservoir ranges from 50 to 150 V/cm. Video images are recorded with a video camera and then digitized. Comparison experiments are done without a granule in the center reservoir but with an electric field.

Figure 3. Images taken at an interval of 12 s when a field of 50 V/cm is applied across the chamber with a cation granule in the center reservoir. Complete mixing of the two dye samples within the center reservoir is achieved within 30 s. The negatively charged cation-exchange granule is seen to move to the junction of its exit channel to the top anode reservoir, and some rattling motion is evident from there the images. Note the continuous dye leakage toward the anode.

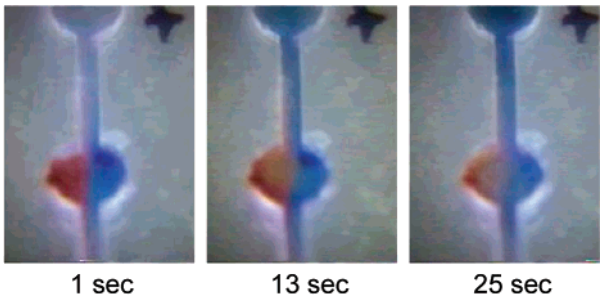

Figure 4. Electrophoretic dye motion toward the anode without mixing action by the granule. Both dye are electrophoretically driven to the exit channel where slight static mixing occurs. Clear color stratification is observed even after several minutes and in the upper reservoir that collects both dyes.

Significant dc electroosmotic flow is observed toward the cathode at the bottom reservoir, indicating the substrate is negatively charged (see Figures 3 and 4). This electroosmotic flow convects both dyes toward the bottom reservoir. In addition, charged dye molecules are observed to exhibit electrophoretic motion of their own. If they are negatively charged for experiments with cation-exchange granules, their electrophoretic direction can be opposite of the electroosmotic convection and moves toward the anode in the upper reservoir. If the exit channel from the center reservoir is initially blocked by one dye because of asymmetric dye placement, some static mixing is observed at the junction with the exit channel as the initial interface between the two dyes is orthogonal to the flow. For this reason, the reference experiment without the granule is carried out with the same electric field to contrast this static mixing to the mixing effected by the nonlinear electrokinetic vortices of the granule.

There is also evidence that a pH gradient develops between the two electrodes because of electrode reactions releasing water electrolysis products, proton and hydroxide ions. In a similar experiment,[16] we have shown that when a dc electroosmotic flow is coupled with a pH gradient, a ζ potential gradient appears to be due to its sensitivity to pH. To maintain constant flow rate, pressure-driven backflow then appears in the high ζ potential region to generate vortices. To visualize the pH gradient and the induced backflow, phenolphthalein indicators were added into solutions to show the concentration profiles of the hydroxide ions. The indicator is clear under neutral and acidic conditions but becomes pink to purple in basic solutions. The

camera begins to record the color change after the dc field (100 V/cm) has been applied for 5 s.

For quantitative characterization of dc mixing, one drop (~1 μL) of each methylene blue-stained and clear glycerin held at the tip of a pipet tip is dipped into the center reservoir, where an anion-exchange granule is placed at the top exit (as seen in Figure 2), as the external voltage is applied. The electric field within the center reservoir ranges from 30 to 125 V/cm. The flux of counterions (anions) into the granule is hence at its bottom half which is within the mixing reservoir. Hence, the vortices and the polarized surface layer due to this flux are confined to the center reservoir.

In contrast, when the granule is positioned at the bottom exit, vortices are not observed within the center reservoir as the polarized side is in the exit channel. The same scenario is observed when the anion-exchange granule moves electrophoretically from the top to the bottom exit. The opposite motion of a cation-exchange granule is seen in Figure 3. Comparison experiments with a passive granule, coated with nail polish to prevent ion flux, positioned at the upstream exit of the mixing chamber or without granule at all are also carried out.

Video images are recorded with a video camera and then digitized. Images are transferred into a personal computer as black-and-white pictures and converted into digital gray scales for each pixel. Gray-scale score statistics transversely across the middle of the center are used to indicate the degree of color heterogeneity. To remove the shadows at the edge, we use only the 40 pixels at the center of the reservoir, which cover more than 90% of the transverse diameter. We compute the gray-scale standard deviation of these pixels, which clearly decreases when the mixing is near completion.

For ac mixing experiments, one cation-exchange granule is placed inside the center reservoir prior to the experiment. Square waveforms at a field strength of approximately ±100 V/cm are applied across the center reservoir. The major difference between ac and dc experiments is that, at low frequencies (<1 Hz), the granule is observed to rattle within the center reservoir.

To obtain extra diffusivity data for ac mixing, glycerin drops stained with anionic dye Rhodamine-6G is used. Experiments and data analyses are similar to those for characterizing dc mixing except ac fields are used.

Nonlinear Electrokinetics Mixing under dc Fields

Without an applied field, the two dye samples within the millimeter-size reservoir take hours to mix by diffusion, as is consistent with our estimate of the diffusion time. This long diffusion mixing time is observed with and without the granule in the mixing reservoir. In contrast, Figure 3 demonstrates the mixing action when an electric field is applied across the reservoir with a fresh granule present. Homogenization occurs within 30 s inside the reservoir. The homogenized mixture is driven electrophoretically out of the reservoir and is also observed in the top channels.

During the short mixing interval, the granule is sometimes observed to move electrophoretically to the junction of its attracting electrode with a high speed of about 1 cm/s. This speed is consistent with earlier measurements in an electrophoretic apparatus.[11] Under some conditions, this displaced granule at the exit channel would rattle in place. It is not clear what mechanism behind the rattling, and it is not always observed. Figure 4 shows the static mixing result with the same applied field but without the granule. Limited static mixing occurs at the junction, but a clear stratification is still apparent in the downstream fluid all the way to the end reservoir. The color segregation persists for 1 h. In an earlier paper,[10] we have shown that static mixing is not efficient in electrokinetic flow because the flat velocity profile minimizes hydrodynamic dispersion. Moreover, mixing by viscous fingering instability is minimal.[12] This instability occurs when a less viscous dye solution is behind a more viscous one at the junction to the exit channel. However, the dominant transverse instability wavelength (the mixing length) exceeds several millimeters and is hence not observed in the current channel or any microfluidic device. Because the field lines are curved within the reservoir and at the junction with the exit channel, some hydrodynamic dispersion can also take place.[13] However, such hydrodynamic mixing only occurs when the stretching action due to streamline curvature is followed by diffusion across the streamlines in the exit channel. The latter diffusion time is again on the order of hours. There is hence little static mixing or hydrodynamic mixing during the experiment. Consistent with these observations, the two colors in Figure 4 are observed to segregate rapidly in the upper channel (exit channel for electrophoretic solute flow) away from the junction. They remain segregated even after they collect at the top reservoir. Little mixing occurs during the long transport to the top reservoir.

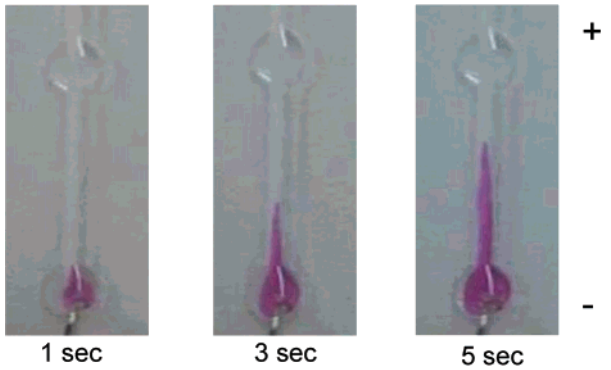

Figure 5. Visualization of the temporal distributions of hydroxide ions generated at the cathode due to electrolysis at 1, 3, and 5 s after the application of electric field. The moving front of hydroxide stream is parabolic, indicating the existence of pH-gradient-induced backflow.

When the field is applied, water electrolysis reactions occur at both electrodes to generate proton and hydroxide ions. Hydroxide ion concentration gradient is visualized by the pink color of phenolphthalein indicators added in solutions (Figure 5).

As the indicators are homogeneously distributed in the channels, the first appearance of pink at the cathode in Figure 5 indicates that the higher pH is higher there and the existence of a pH gradient between the electrodes. However, as the electroosmotic flow is from the anode to cathode, the pink indicators should be confined to the cathode reservoir without convection leakage out. However, Figure 5 clearly indicates a parabolic convective flow profile of the pink indicator from the cathode to the anode. This indicates significant pressure-driven backflow in the opposite direction of electroosmotic flow due to the pH gradient.

As the dissociation of surface carboxylate group is pH dependent,[15] the pH gradient from the electrolysis causes nonuniform ζ potential along the channel.[16] In particular, the higher pH cathode region should have a higher electroosmotic slip velocity toward the anode than the lower pH anode region. This slip velocity gradient can only be commensurate with constant flow from the anode to the cathode if a slender vortex pair appears at the high-slip anode region because of pressure-driven backflow away from the walls. Within the vortex region, the flow is parabolic with the tip velocity toward the anode and the surface velocity toward the cathode. This is clearly consistent with the phenolphthalein pink indicators at the bottom images of Figure 5. We hence have a slender vortex pair generated by pressure-driven backflow at the anode end. With a sufficiently large pH gradient, this slender vortex can span the entire length between two electrodes.

How this back-pressure-driven slender vortex pair couples with the nonlinear vortex pair of the granule is evident in Figure 6. There an anion-exchange granule is affixed to the top anode end of the mixing reservoir such as its nonlinear vortices are inside the mixing reservoir. We note from Figure 6 that the flow field of this vortex pair near the granule surface is from the pole to the equator. The slender back-pressure-driven vortex pair is also sketched in Figure 6. Notice that the two vortex pairs have the same rotational directions and hence cannot coexist in steady state. From the two images in Figure 6, it is clear that dye placed on one side of the reservoir is injected into the cathode channel by electroosmotic flow but reejected into the reservoir by the back-pressure-driven flow such that it lies on the opposite side of the main channel. This injection−rejection mechanism clearly suggests a slender vortex within the cathode channel.

Intense and nonsteady flows exist within the mixing reservoir. As the two vortex pairs are incommensurate at steady state, extremely transient mixing flow exits between them. Microscope visualization of microsize latex particles in this region also indicate global turbulent like fluctuations exist in the reservoir. In contrast, in the unbounded reservoir of Figure 1, the vortex pair is localized and steady. The coupling of the nonlinear vortex pair hence produces extremely effective nonsteady mixing vortices.

Without an applied field, the colored glycerin within the milimeter-size reservoir takes almost 30 min to diffuse over the reservoir, as is consistent with our estimate of the diffusion time. The curve of gray-scale standard deviation versus time show the mixing action quantitations when electric field 100 V/cm is applied across the reservoir with a fresh anion-exchange granule present at the upper exit. The normalized concentration within a reservoir is expected to approach a homogeneous field exponentially if only diffusion at play. The exponent is $-Dt/l^2$ multiplied by a unit-order factor, where $l = 3$ mm is the diameter of the reservoir. Hence, a measure of our mixing efficiency can be obtained by assuming a purely diffusive mechanism. As such, the mixing diffusivity can be derived via the linear regression of the logarithm value of standard deviation against time (Figure 7). The slope of this curve scales linearly with respect to the diffusivity coefficient. The regressed slope from the data of ion diffusion without electric field, when divided by l^2, yields a diffusivity D_0 that is close to the usual ion diffusivity of 10^{-5} cm^2/s. However, because we do not use the all the pixels within the reservoir and because the concentration field may not be two-dimensional (independent of the depth), this may not present an accurate estimate of the true diffusivity.

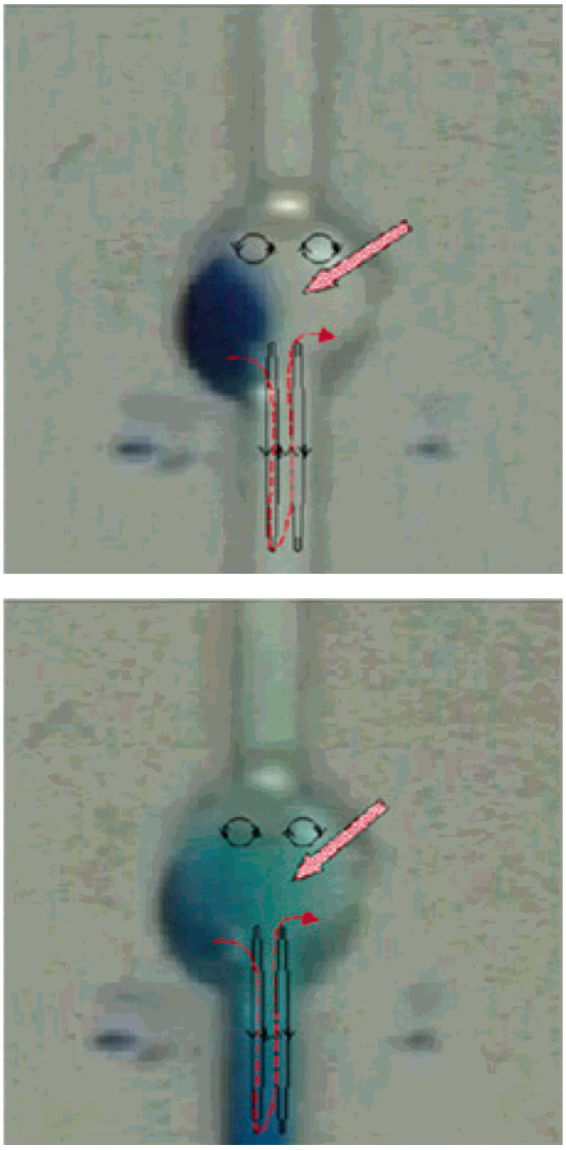

Figure 6. Two images taken at 1 and 17 s for an anion-exchange granule. The vortex pair at the granule and the other vortex pair at the bottom cathode junction are sketched. The dye placed on the side is injected and reejected from the cathode junction by the latter vortex pair. The arrows indicate the regions where turbulent streamlines are observed under the microscope.

As such, we divide the slope of the fitted straight lines in Figure 7 by the slope of the curve of the fieldless data to estimate a normalized effective diffusivity, as the straight curves in Figure 7 indicate that the mixing in the reservoir can be accurately represented by a diffusing mixing model with an effective mixing diffusivity D_{eff}. The normalized mixing diffusivity hence represents the effects of electrokinetic flow on mixing relative to the case without flow.

Similarly, mixing diffusivity coefficients are obtained in comparison experiments. The results of all diffusivity coefficients are shown in Figure 8, the log−log plot of mixing diffusivity dependence on field strength.

Figure 8 shows almost 2 orders of magnitude enhancement of diffusivity at the electric field 125 V/cm

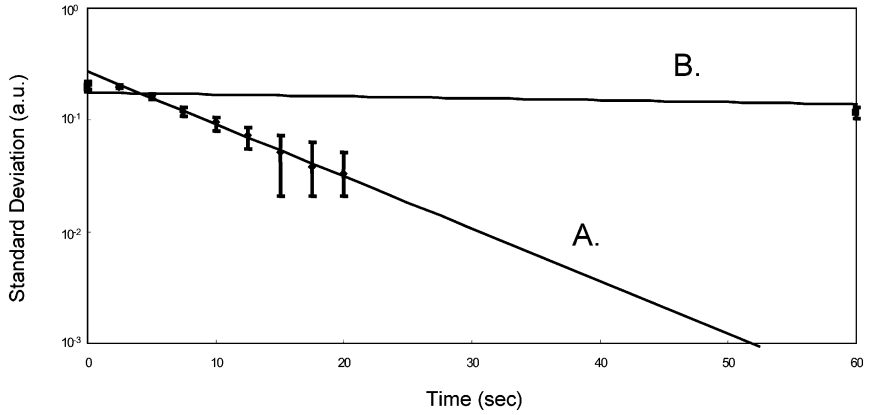

Figure 7. Mixing action quantitation obtained from the global temporal change of standard deviation of gray-scale scores of camera pixels imaging mixing action inside the reservoir. The mixing diffusivity (curve A) for an anion-exchange granule at 100 V/cm is compared to that without a field (curve B).

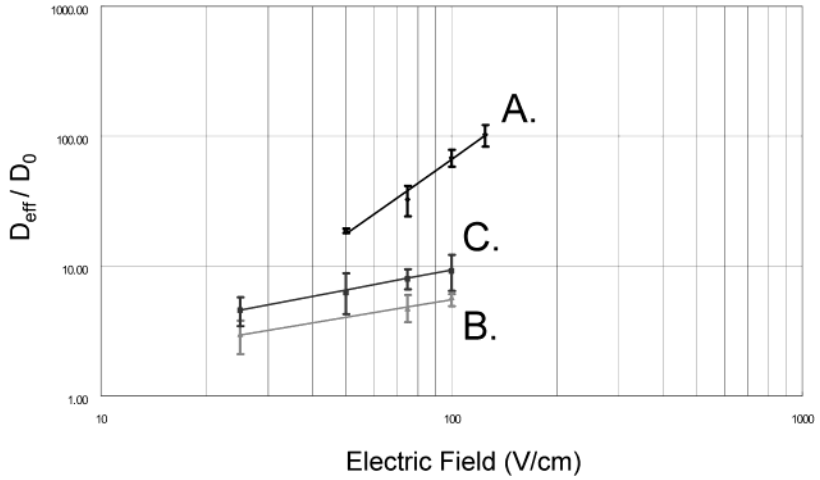

Figure 8. log−log plot of mixing diffusivity dependence on field strength. The half range of the error bar of each point is twice that of slope standard deviations estimated via regressed linear curves similar to Figure 7. Curve A shows mixing diffusivity scales to $E^{1.9\pm0.3}$ (E: field strength) when fresh granule is present in the reservoir. Curves B and C show mixing diffusivity scales to $E^{0.45\pm0.07}$ and $E^{0.50\pm0.02}$, respectively, when passive granule or no granule is present.

when nonlinear electrokinetics, that is granule-generated vortices, exists. Two comparison experiments using either passive granule or no granule indicate more or less the same mixing effect. The geometric effect due to the presence of the granule proves to be insignificant. The contributions due to linear electrokinetics, that is, mixing by the slender vortices due to a combination of channel electroosmosis and the pH-gradient-induced backflows, is less significant than that due to vortices by a factor of 10 but still several factors higher than pure diffusion.

In Figure 8, curve A yields a power of 1.9 ± 0.3 with respect to E, which indicates the mixing diffusivity is approximately dependent on the square of field strength. This result is consistent with the trends of vortex speed predicted in our previous theoretical studies.[9,10] Curves B and C have almost identical slopes 0.45 ± 0.07 and 0.50 ± 0.02, respectively. These small slope values also suggest the weak dependence of mixing action on field strength, when the mixing is due to pH-induced ζ potential differences. As the field strength increases, mixing diffusivity enhancement should be mainly due to the nonlinear electrokinetics of ion-exchange granules. Nevertheless, the pH-induced backflow is essential in breaking up the former vortices. From Figure 5 and related measurements, we estimate the velocity due to pressure-driven backflow to be a small ~1 mm/s. Nevertheless, it is sufficient to produce turbulent-like unsteady mixing for microfluidic devices!

Nevertheless, the electroosmotic flow and pressure-driven backflow of the dc case has a distinct undesirable characteristic. The dye is convected out of the mixing reservoir, as seen in Figures 3 and 4. Such a disadvantage is removed by ac mixing.

Nonlinear Electrokinetics Mixing under ac Fields

Figure 9 shows the mixing action images taken at 1, 5, 15, and 30 s after the square waveform ac electric field (0.3 Hz; $E_{rms} \sim 100$ V/cm) is applied across the mixing chamber. Two segregated ink dyes were mixed homogeneously within 30 s. The granule is clearly observed to rattle within the chamber at this low frequency. The rattling ceases beyond 1 Hz. Unlike dc fields, there is no net electroosmotic flow, net electromigration ions, and net electrophoretic particle motion. As such, in contrast to the dc case of Figures 4 and 5, dye solutions do not disperse far away from the mixing chamber. In Figure 10, the images are taken at 15 s after the electric fields with 1, 10, 100, and 10 000 Hz are applied, respectively. Although dye solutions are mostly confined to the chamber, the mixing action becomes less intense as the field frequency increased to faster than 1 Hz.

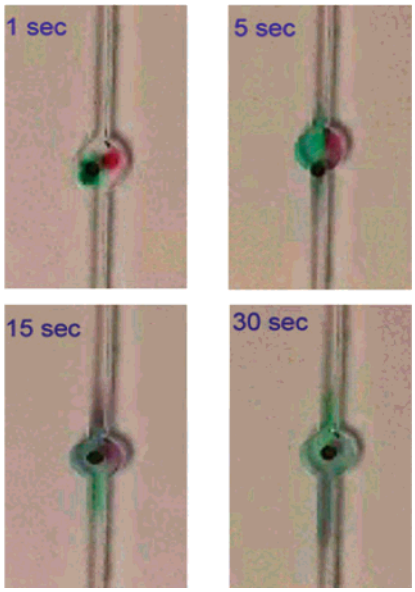

Figure 9. Mixing action using nonlinear electroosmosis produced by square waveform ac field (0.3 Hz; −100 to +100 V/cm; duty cycle 50%). Two segregated ink-dye solutions are mixed homogeneously within 30 s.

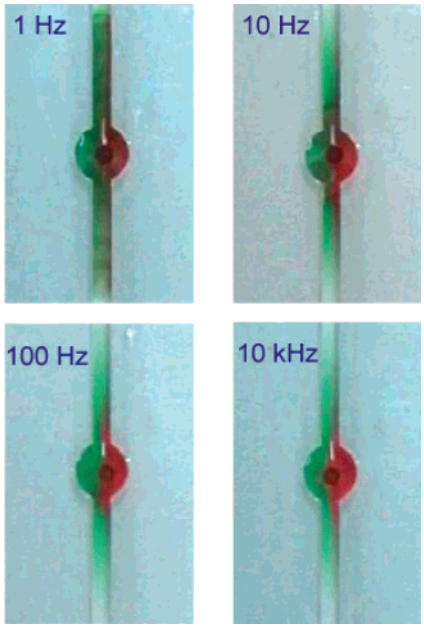

Figure 10. Mixing action using ac field nonlinear electroosmosis (square waveform; − 130 to +130 V/cm; duty cycle 50%) at 30 s after the field is applied. Mixing actions became significantly attenuated at frequency higher than 10 Hz.

Mixing action at frequency lower than 0.3 Hz is similar to those with a dc electric field (images not shown). Dye solutions are mixed within 0.5 min but are also driven toward or even into the side reservoirs by the electrophoretic flows. The electroosmotic convection time across the channel is apparently less than 10 s. This corresponds to a rather high linear electrokinetic velocity of 1 mm/s, consistent with our estimate from dc experiments from Figure 5.

Coupled with granule's electrophoretic rattling, microvortices generated by nonlinear electrokinetics around the granule are continuously broken and re-formed on the opposite side, giving rise to a highly transient vortex flow. Intense chaotic mixing actions were clearly seen with two originally separated dyes. Frequencies lower than the inverse translation time of the granule would yield granule trajectories that are affixed to the end of the reservoir for a large fraction of the period. The frequency should also be lower than a critical value such that the ions have sufficient time to migrate into the double layer within a half cycle to produce the nonlinear electrokinetic vortices of Figure 1. These considerations and the constraint that the dye molecules being mixed should remain within the chamber produce a narrow window of frequencies where all these mechanisms resonate to produce maximum mixing. This window in frequency is estimated experimentally by a sequence of experiments shown in Figure 10. The mixing actions remain intense when the ac field frequency is less than 1 Hz. When the frequency exceeds 1 Hz, granules do not traverse visibly inside the chamber. There are several possible explanations for this suppression of granule motion. The diffusion time scale around the granule is around 1 s, and it could be the polarization across the granule has been neutralized by diffusion. Any rotational motion of the granule must require a nonuniform polarization, and granule rotation also ceases. Finally, the linear electrophoretic displacement of the granule decreases with increasing frequency and the granule simply does not move appreciably but retains its polarization. We observe that the microvortex streamlines persist even after the linear granule motion ceases. This suggests that the granule remains polarize but the linear displacement becomes negligible.

Optimum mixing requires both granule motion and vortices produced by polarization. Hence, frequencies lower than 1 Hz should be employed. However, the electromigration speed of ions is much higher than the electrophoretic speed of the granule. Hence, too low a frequency would lead to excess leakage of the dye out of the chambers. Because of these tradeoffs, we estimate the optimum ac field frequency to be 0.3−1 Hz but this value would be a function of the granule and chamber size.

In Figure 11, normalized mixing diffusivity dependence on applied field frequency show the mixing effects described in the above quantitatively. Furthermore, each plateau (relaxation) of this curve is consistent with the predicted time scaling of mixing types. First, as discussed in the above, the most intense mixing occurs at the combination of electrophoretic motion of granules and vortices. The largest mixing diffusivity exists at the range 0.1−1 Hz. Next, although the electrophoretic speed of granule is about cm/s, no visible displacement would appear when the ac frequency is higher than 10 Hz. In other words, at frequencies higher than 10 Hz, mixing action would be solely provided by the vortices, as the granule displacement stops. As shown in Figure 11, the mixing diffusivity drops from 10^{-3} to 10^{-4} cm^2/s when the ac frequency is tuned from 1 to 10 Hz. Also, at these high frequencies, electrolysis products do not have sufficient time to travel out off the side reservoirs to generate pH-gradient-induced backflows. The mixing action above 10 Hz should have no contribution from pH-induced backflows. Finally, the vortices are supposed to cease when ions do not have enough time to diffuse across the Debye layer. The mixing diffusivity is predicted to drop to the order of ion diffusivity when frequency is about 10−100 kHz (D/λ^2; D = ion diffusivity; λ = Debye layer thickness). We have observed the

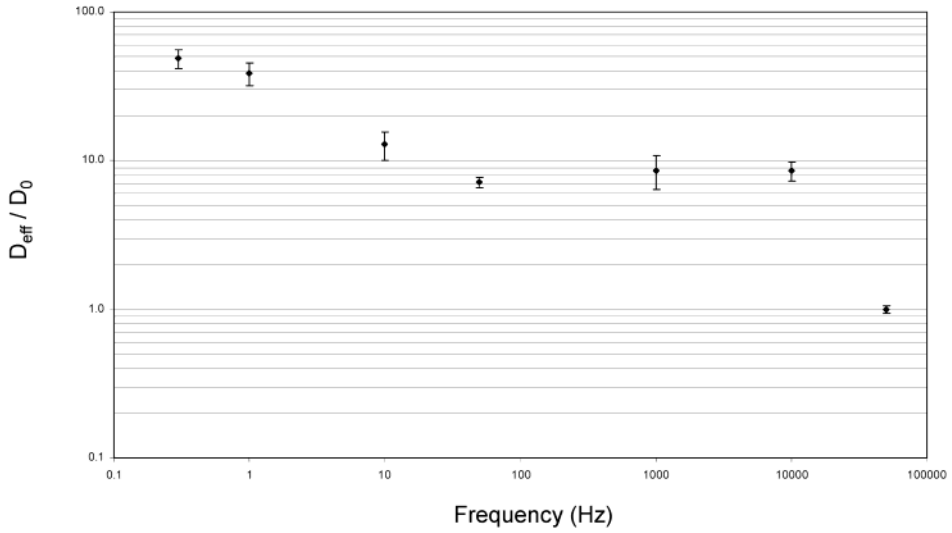

Figure 11. Normalized mixing diffusivity dependence on ac frequency of applied electric field at 100 V/cm.

evidence of vortex termination at 50 kHz as the normalized mixing diffusivity decreases to that without an applied field.

Conclusions

Effective mixing 2 orders of magnitude higher than molecular diffusion has been achieved in a small size reservoir (less than 10 μL) with turbulent-like flows at a through-flow Reynolds number of less than 1. These chaotic and turbulent mixinglike flows are created when nonlinear electroosmotic microvortices couple with the nonlinear electrophoretic rattling of the granule in an ac field and with pressure-driven backflow in a dc field. The latter secondary flows act to break up the intense microvortices to allow solute transport into the intense mixing region within the vortices. The microvortices resulted from fluid circulation created by nonuniform polarization of one ion-specific granule inserted in an electric field (30−125 V/cm). The applicability of this unique mixing mechanism was demonstrated under moderate electric fields and without flow splitting by baffles or mechanical stirrers with moving parts. Although diffusive mixing would take more than 1 h for the low diffusivity dye, the new mechanism is able to achieve complete mixing in 30 s corresponding to a 2-order reduction in mixing time.

Although there is only one mixing chamber in our device, replicating hundreds of them on one substrate disk should be a straightforward fabrication effort. Electrodes can be fabricated by depositing conductive materials on the edge of the reservoirs. Similar designs can be envisioned for wet-well/micropipet arrays, where one electrode is at the wet well and one at the tip of the pipet dispensing the solution. If the granules are predeposited into the wet wells by the pipet array or inserted into the reactant solution directly, the mixing action can initiate the instant the final reactants are released into the wet wells. Scaling down to microfluidic mixing chambers smaller than 100 μm needs to be done with care. Granules smaller than 100 μm in diameter tend to saturate more rapidly and have slower nonlinear electrophoretic velocities. Instead, patterned channel walls made out of ion-specific porous material may be preferred. If the dc electric field is supplied by internal electrodes within an enclosed microfluidic device, bubble generation can also be problematic.

Although the dc mixing is competitive against ac mixing, when Figure 6 is compared to Figure 9, there is a clear advantage for using an ac field. First of all, the pH gradient may not be sufficiently strong for a long channel to produce intense dc mixing. Also electrode reaction releasing bubbles and contaminants can be minimized with a sufficient high-frequency ac field whose period is longer than the diffusion time but shorter than the reaction time. Most importantly, with a sufficient high frequency (1 Hz in the current setup), the solute to mixed is confined to the mixing chamber with an ac field, as seen in Figures 9 and 10. Even with further improvements and other more detailed design considerations, simple fabrication and the intense mixing action are major advantages for the current nonlinear electrokinetic mechanism.

Acknowledgment

This work is supported by the Center for Microfluidics and Medical Diagnostics of the University of Notre Dame and by NASA. The authors thank D. T. Leighton of the Center for his input on dc mixing mechanisms. The image of Figure 1 was taken by P. Takhistov, formerly of our group. S.-C.W. and Y.-W.L. also acknowledge the research financial support by National Science Council, Taiwan, and the National Chung Cheng University.

Literature Cited

(1) Schwesinger, N.; Frank, T.; Wurmus, H. A Modular Microfluid System with an Integrated Micromixer. *J. Micromech. Microeng.* **1996**, *6*, 99.

(2) Jacobson, S. C.; Mcknight, T. E.; Ramsey, J. M. Microfluidic Devices for Electrokinetically Driven Parallel and Serial Mixing. *Anal. Chem*. **1999**, *71*, 4455.

(3) Thamida, S.; Chang, H.-C. Nonlinear Electrokinetic Ejection and Entrainment due to Polarization at Nearly Insulated Wedges. *Phys. Fluids* **2002**, 4315.

(4) Oddy, M. H.; Santiago, J. G.; Mikkelsen, J. C. Electrokinetic Instability Micromixing. *Anal. Chem*. **2001**, *73*, 5822.

(5) Johnson, T. J.; Ross, D.; Locascio, L. E. Rapid Microfluidic Mixing. *Anal. Chem*. **2002**, *74*, 45.

(6) Probstein, R. F. *Physiochemical Hydrodynamics*; John Wiley & Son: New York, 1994.

(7) Dukhin, S. S. Electrokinetic Phenomena of the Second Kind and Their Applications. *Adv. Colloid Interface Sci*. **1991**, *35*, 173.

(8) Mishchuk, N. A.; Takhistov, P. V. Electroosmosis of the Second Kind. *Colloids Surf., A* **1995**, *95*, 119.

(9) Ben, Y.; Demekhin, E. A.; Chang, H.-C., Nonlinear Electrokinetics and "Super-fast" Electrophoresis. Accepted for publication in *J. Colloid Interface Sci*.

(10) Ben, Y.; Chang, H.-C. Nonlinear Smoluchowski Velocity and Micro-vortex Generation. *J. Fluid Mech*. **2002**, *461*, 229.

(11) Barany, S.; Mishchuk, N. A.; Prieve, D. C. Superfast Electrophoresis of Conducting Dispersed Particles. *J. Colloid Interface Sci.* **1998**, *207*, 240.

(12) Ben, Y.; Demekhin, E. A.; Takhisov, P. V.; Chang, H.-C. Miscible Fingering in Electrokinetic Flow. *J. Chin. Inst. Chem. Eng.* **2002**, *33*, 15−24.

(13) Dutta, D.; Leighton, D. T. A Low Dispersion Geometry for Microchip Separation Devices. *Anal. Chem*. **2002**, *74*, 1007.

(14) Ghosh, S.; Chang, H.-C; Sen, M. Heat Transfer Enhancement due to Slender Recirculation and Chaotic Transport Between Counter-Rotating Eccentric Cylinder. *J. Fluid Mech*. **1992**, *238*, 119.

(15) Wang, S.-C.; Perso, C. E.; Morris M. D. Effects of Alkaline Hydrolysis and Dynamic Coating on the Electroosmotic Flow in Polymeric Microfabricated Channels. *Anal. Chem*. **2000**, *72*, 1704.

(16) Minerick, A. R.; Ostafin, A. E.; Chang, H.-C. Electrokinetic Transport of Red Blood Cells in Microcapillaries. *Electrophoresis* **2002**, *23*, 2165.

Received for review September 2, 2003
Revised manuscript received January 28, 2004
Accepted January 29, 2004

IE030689R